Decline in terrestrial moisture sources of the mississippi river basin in a future climate

Benedict, Imme; Van Heerwaarden, Chiel C.; Van Der Ent, Ruud J.; Weerts, Albrecht H.; Hazeleger, Wilco

DOI
10.1175/JHM-D-19-0094.1

Publication date
2020

Document Version
Final published version

Published in
Journal of Hydrometeorology

Citation (APA)
Benedict, I., Van Heerwaarden, C. C., Van Der Ent, R. J., Weerts, A. H., & Hazeleger, W. (2020). Decline in terrestrial moisture sources of the mississippi river basin in a future climate. *Journal of Hydrometeorology*, *21*(2), 299-316. https://doi.org/10.1175/JHM-D-19-0094.1

Decline in Terrestrial Moisture Sources of the Mississippi River Basin in a Future Climate

IMME BENEDICT AND CHIEL C. VAN HEERWAARDEN

Meteorology and Air Quality Group, Wageningen University, Wageningen, Netherlands

RUUD J. VAN DER ENT

Department of Water Management, Faculty of Civil Engineering and Geosciences, Delft University of Technology, Delft, and Department of Physical Geography, Faculty of Geosciences, Utrecht University, Utrecht, Netherlands

ALBRECHT H. WEERTS

Deltares, Delft, and Hydrology and Quantitative Water Management Group, Wageningen University, Wageningen, Netherlands

WILCO HAZELEGER

Meteorology and Air Quality Group, Wageningen University, Wageningen, and Faculty of Geosciences, Utrecht University, Utrecht, Netherlands

(Manuscript received 29 April 2019, in final form 30 October 2019)

ABSTRACT

Assessment of the impact of climate change on water resources over land requires knowledge on the origin of the precipitation and changes therein toward the future. We determine the origin of precipitation over the Mississippi River basin (MRB) using high-resolution (~25 km) climate model simulations for present and future climate (RCP4.5). Moisture resulting in precipitation over the MRB is tracked back in time using Eulerian offline moisture tracking, in order to find out from where this water originally evaporated (i.e., the moisture sources). We find that the most important continental moisture sources are the MRB itself and the area southwest of the basin. The two most relevant oceanic sources are the Gulf of Mexico/Caribbean and the Pacific. The distribution of sources varies per season, with more recycling of moisture within the basin during summer and more transport of moisture from the ocean toward the basin in winter. In future winters, we find an increase in moisture source from the oceans (related to higher sea surface temperatures), resulting in more precipitation over the MRB. In future summers, we find an approximately 5% decrease in moisture source from the basin itself, while the decrease in precipitation is smaller (i.e., lower recycling ratios). The results here are based on one climate model, and we do not study low-frequency climate variability. We conclude that Mississippi's moisture sources will become less local in a future climate, with more water originating from the oceans.

1. Introduction

The atmospheric water budget is affected by climate change. Precipitation is expected to increase at high latitudes and around the equatorial band (Gimeno et al. 2012; Trenberth 2011), and a reduction is expected in subtropical subsidence regions (Allen and Ingram 2002). Changes in mean annual evaporation follow the changes in temperature (Held and Soden 2006), with increasing evaporation rates over most of the oceans (Gimeno et al. 2012). Higher temperatures in a future climate also result in more atmospheric water vapor in the lower troposphere following Clausius–Clapeyron, amplifying the atmospheric water cycle (Held and Soden 2006). Besides thermodynamic effects, changes in circulation

Denotes content that is immediately available upon publication as open access.

Corresponding author: Imme Benedict, imme.benedict@wur.nl

DOI: 10.1175/JHM-D-19-0094.1

patterns can affect the atmospheric water budget on a regional level. Both dynamic (circulation) and thermodynamic effects are relevant when considering moisture sources of a region, that is, the evaporative sources resulting in precipitation over a defined area.

Hydrological basins are often used as study areas on a regional level, since changes in the atmospheric water cycle also influence discharge and soil moisture characteristics, which are important for water management. In addition, the origin of the precipitation, being continental or oceanic, can indicate the vulnerability of a basin to ongoing and future land-use changes. Furthermore, the location of the sources can also indicate whether there is a greater need to improve the model representation of ocean or land evaporation.

So far, moisture source regions are mostly determined for present climate (Algarra et al. 2019; Bosilovich and Chern 2006; Bosilovich and Schubert 2001; Brubaker et al. 2001; Dirmeyer and Brubaker 1999; Knoche and Kunstmann 2013; Sodemann et al. 2008; Stohl and James 2005). Consequently, one of the remaining questions in atmospheric moisture transport was stated in the review by Gimeno et al. (2012): ''How will climate change alter the location and significance of source regions and the transport of moisture from these toward continental areas in the future?'' Here, we focus on the atmospheric water budget and the moisture sources of the Mississippi River basin (MRB) and how these are affected by climate change.

The Mississippi River basin is the fourth-largest river basin in the world, and it contains one of the world's most productive agricultural regions (the Corn Belt). In addition, it is an important source of water to millions of people, as well as industry. Therefore, it is important to understand its hydrological cycle and the local variations therein. The precipitation budget of the MRB is influenced by moisture input from multiple drivers. Moisture is advected from the Pacific over the western boundaries of the MRB, resulting in high precipitation amounts and snow over the Rocky Mountains, mainly in winter. At the southern boundary, moisture is advected from the warm tropical Atlantic, Caribbean, and the Gulf of Mexico resulting in relatively wet conditions in the southeast. A large set of climate models indicates that in the future those wet regions (southeast and Rocky Mountains) get wetter [CMIP3 (Seager et al. 2010) and CMIP5 (Seager et al. 2013)]. In summertime, moisture transport is related to the Great Plains low-level jet (LLJ), ranging from the Gulf of Mexico inlands (Algarra et al. 2019; Helfand and Schubert 1995; Higgins et al. 1997). This supply of moisture, together with large surface fluxes results in convective precipitation in summer over the MRB.

In present climate, moisture sources and moisture recycling of the MRB is widely studied. First research was conducted by Benton et al. (1950), who studied the different (continental and maritime) air masses bringing precipitation over the river basin. Benton et al. (1950) concluded that 10% or less of the precipitation over the Mississippi had its evaporative sources from within the basin, where Brubaker et al. (1993) found recycled fractions ranging between 20% and 30% depending on the season. Later, Brubaker et al. (2001) determined from a long climatology (36 years) of warm-season precipitation that 32% of the moisture source originated from the MRB itself and about 20% from the Gulf of Mexico. Further, the establishment of anticyclonic flow around the Bermuda high, a high pressure system over the Atlantic during summer, lengthens the fetch of moisture sources from the Gulf of Mexico/Atlantic Ocean into the Caribbean and tropical Atlantic. In the project by Dirmeyer et al. (2009), a climatology of moisture sources per basin, including the Mississippi, were determined and visualized. Over time, other moisture tracking methods were suggested and applied to the MRB, for example the use of passive tracers (Bosilovich and Schubert 2002; Bosilovich and Chern 2006) and a Lagrangian tracking method (Stohl and James 2005). The latter found similar moisture sources for the MRB as Brubaker et al. (2001). Recently, a moisture tracking model was used to explore the role of reduced moisture transport in drought propagation over North America (Herrera-Estrada et al. 2019).

All studies mentioned above assess the moisture sources and moisture recycling of the MRB/North America for present climate, because moisture tracking is mostly applied to atmospheric reanalysis datasets. However, reanalyses do not provide information on the future. As a consequence, one of the open questions in the field of atmospheric moisture transport is how moisture sources are affected by climate change (Gimeno et al. 2012; Guo et al. 2019). Findell et al. (2019) studied continental precipitation under rising temperatures on a global scale, and emphasized the need to further study regions such as the corn producing regions of North America, given their importance for agriculture. Gimeno et al. (2013) detected regions of continental precipitation which are vulnerable to changes in oceanic moisture sources (i.e., changes in evaporation). They selected regions where climate change will likely lead to an increase in evaporation minus precipitation (so-called hot spot regions) and performed forward tracking of moisture to identify which continental regions were affected by these hot spot source regions. Ideally, a tracking algorithm should be applied directly

to simulations of future climate using a global climate model (Gimeno et al. 2013), which is what we do in this study.

We use 30-yr high spatial resolution (~25 km) simulations of a global climate model for present and future climate [representative concentration pathway 4.5 (RCP4.5); van Vuuren et al. 2011]. We choose to use high-resolution global simulations as this benefits the representation of, among others, El Niño–Southern Oscillation (ENSO; Shaffrey et al. 2009), the global water cycle (Demory et al. 2014), storm tracks (Hodges et al. 2011), and cyclones (Strachan et al. 2013). At the expense of the high resolution, the simulations have a limited simulation length (six members of 5 years per period), and therefore we cannot study multidecadal variability. We focus on the mean change of the different terms of the atmospheric water budget, and Mississippi's moisture sources. Our two main research questions are stated as follows: 1) How is the modeled atmospheric water budget over the Mississippi River basin projected to change in the future? 2) How will climate change alter the relative contribution of the oceanic and terrestrial moisture source regions of the Mississippi River basin?

We structure the paper as follows. We start with the theory on atmospheric water vapor tracking and we define the evaporation recycling ratio (section 2). In the methodology (section 3), we describe the data from the climate model EC-Earth, the tracking model Water Accounting Model-2layers (WAM-2layers), and our experimental setup. In section 4, we validate precipitation and evaporation from EC-Earth and analyze how it is changing toward the future. Thereafter (section 5), we validate the use of WAM-2layers with the EC-Earth data. In section 6, we show and discuss the moisture sources of the MRB in present and future climate, and their seasonal variation. Finally, we discuss the methodology, and we end with a summary and conclusions.

2. Theory on atmospheric moisture tracking and recycling ratios

Moisture is added to the atmosphere via evaporation E, it is transported by the wind, and becomes a loss term in the atmospheric water budget as precipitation P. Here, we follow the notation of van der Ent et al. (2010, 2014) to define the atmospheric water budget:

$$\frac{\partial S}{\partial t} + \frac{\partial F_x}{\partial x} + \frac{\partial F_y}{\partial y} = E - P, \tag{1}$$

where $S = (1/\rho_w g)\int_0^{p_s} q\, dp$, $F_x = (1/\rho_w g)\int_0^{p_s} (qu)\, dp$, $F_y = (1/\rho_w g)\int_0^{p_s} (qv)\, dp$, ρ_w is the density of water, g is the gravitational constant, p_s is the surface pressure, 0 indicates the pressure at the top of the atmosphere, q is specific humidity, and u and v are the wind components in the east–west and north–south directions, respectively. When we determine the moisture budget over a longer time period, the change of atmospheric water vapor over time is negligible and the first term in Eq. (1) can be neglected.

When moisture is tracked from its source (evaporation over a region) to its sink (precipitation) Eq. (1) can be adapted as follows, indicating forward tracking:

$$\frac{\partial S_m}{\partial t} + \frac{\partial F_{x,m}}{\partial x} + \frac{\partial F_{y,m}}{\partial y} = \delta E + P_m, \tag{2}$$

where the m indicates the tracked moisture and the δ indicates the source area of interest.

Here, we are mostly interested in the moisture sources which bring precipitation to a defined region. To determine these moisture sources, moisture is tracked backward in time, which means that precipitation becomes the source and evaporation the sink. Therefore, E and P switch sign compared to the forward tracking:

$$\frac{\partial S_m}{\partial t} + \frac{\partial F_{x,m}}{\partial x} + \frac{\partial F_{y,m}}{\partial y} = -E_m + \delta P. \tag{3}$$

In this study, $\delta = 1$ inside the MRB and $\delta = 0$ outside the MRB. The term E_m is the source of the tracked moisture and is shown through this study as the resulting moisture source.

When tracking moisture backward in time, we can determine the ratio between evaporation moisture source summed over the region (A) and the total evaporation summed over the region, which we call the evaporation recycling ratio ϵ_r:

$$\epsilon_r = \frac{\int_A \delta E_m\, dA}{\int_A \delta E\, dA}. \tag{4}$$

3. Methodology

a. Model data: EC-Earth

We use simulations with high spatial resolution (Haarsma et al. 2013) from the atmospheric global climate model EC-Earth V2.3 (Hazeleger et al. 2010, 2012). The runs have a horizontal spectral resolution of T799 (~25 km) and 91 vertical levels. The EC-Earth model is based on the European Centre for Medium-Range Weather Forecasts numerical weather prediction model Integrated Forecasting System (IFS) cy31r1. An improved hydrology scheme (H-TESSEL; Balsamo et al. 2009; van den Hurk

et al. 2000) is inserted in EC-Earth. Actual evaporation is computed by this scheme using a tile approach, such that each grid cell can contain multiple land-use types.

The experiment consists of six members of 5 years for present climate (2002–06) and future climate (2094–98), resulting in a dataset of 30 years for each period. A 10-yr spin up run at low resolution (T159) was made for both the present and the future, followed by a 9-month (from January to October) spinup run at T799 resolution. The six-member ensemble was made by taking the atmospheric state of one of the first 6 days of October as initial state for each member. Thereafter, the model was run for another 3 months until 1 January before the data were used for the analysis. After this spinup the spread in the atmospheric states was sufficient to treat the six runs as independent members (Haarsma et al. 2013).

In the present-day simulations, observed greenhouse gases and aerosol concentrations were applied, while future concentrations were derived from the RCP4.5 scenario (van Vuuren et al. 2011). Sea surface temperatures (SSTs) were imposed using daily data at 0.25° horizontal resolution from NASA (http://www.ncdc.noaa.gov/oa/climate/research/sst/oi-daily.php) for the 2002–06 period. The SSTs for the future were calculated by adding the projected ensemble mean change using the 17 members of the coupled climate model ECHAM5/MPI-OM in the ESSENCE project (Sterl et al. 2008) under the SRES A1B emission scenario (Nakićenović and Swart 2000). This scenario is compatible with the RCP4.5 scenario, but the median global temperature increase by the end of the twenty-first century is about 1°C smaller (Rogelj et al. 2012). Further details on model setup can be found in Haarsma et al. (2013) and Baatsen et al. (2015).

We obtain the following variables from the model: evaporation $E(t, x, y)$, precipitation $P(t, x, y)$, surface pressure $p_s(t, x, y)$, the two horizontal wind components at 10 m u10(t, x, y) and v10(t, x, y), dewpoint temperature at 2 m d2m(t, x, y), specific humidity in the atmosphere $q(t, x, y, p)$, and the two wind components in the atmosphere $u(t, x, y, p)$ and $v(t, x, y, p)$. Specific humidity at the surface is derived from dewpoint temperature at 2 m and surface pressure. Surface data is available at a 3-hourly time step and atmospheric data at a 6-hourly time step. One important constraint of the EC-Earth data compared to reanalysis data is that the atmospheric variables are only saved at five pressure levels in the atmosphere, namely, 850, 700, 500, 300, and 200 hPa.

b. *Validation data: ERA-Interim, CMIP5, and observations*

We compare E and P from EC-Earth with other model simulations of the Atmospheric Model Intercomparison Project (AMIP) CMIP5 (Taylor et al. 2012) from 1979 to 2008 for present climate, and from 2070 to 2100 for future climate based on the RCP4.5 scenario. This project also includes simulations with EC-Earth, although with a different setup and lower resolution than the climate runs we perform the tracking for. Furthermore, we use reanalysis data from ERA-Interim (1985–2014; Dee et al. 2011) and ERA-Interim/Land (1985–2010; Balsamo et al. 2013). We also include observational data of the Climate Prediction Center (CPC) 0.25° Daily U.S. Unified Gauge-Based dataset version 1.0 (1985–2014; Higgins et al. 2000) for precipitation and the GLEAM dataset (1985–2014; Martens et al. 2016) for evaporation.

For validation of the moisture tracking, we force the tracking model WAM-2layers with ERA-Interim reanalysis data (Dee et al. 2011). ERA-Interim (ERAI) provides atmospheric information (specific humidity and wind) at both model levels and pressure levels. The atmospheric data has a 6-hourly time step and the surface data a 3-hourly time step. For this validation, we obtain the ERAI data with a horizontal resolution of 1.5° × 1.5° for the year 2002.

c. *Tracking method: WAM-2layers*

We use WAM-2layers (van der Ent et al. 2010, 2014) to determine the moisture sources of the MRB. WAM-2layers is an Eulerian offline moisture tracking model which solves the atmospheric water balance [Eq. (1)] for every grid cell. The model can perform both forward and backward moisture tracking. We primarily use backward tracking to determine the moisture sources of the MRB [Eq. (3)]. WAM-2layers performs the tracking in two layers in the atmosphere, hence the atmospheric information is integrated to two layers (van der Ent 2014). The model assumes well-mixed conditions in both layers [$P_k = P \times (S_k/S)$] and evaporation only contributes to the lower layer. Transport of moisture between the layers can occur via vertical component F_v. The vertical transport F_v between the two layers is determined from closing the water balance between the two layers. Furthermore, to take into account the nonclosure of the data, a sigma term σ_k is added:

$$\frac{\partial S_{m,k}}{\partial t} + \frac{\partial F_{x,m,k}}{\partial x} + \frac{\partial F_{y,m,k}}{\partial y} = \delta P_k - E_{m,k} + F_v + \sigma_k, \quad (5)$$

where k indicates either the bottom or the top layer. The division between the two layers depends on the surface pressure: $p_{\text{divide}} = 7438 + 0.72p_s$ (Pa). For more information on the model we refer to van der Ent (2014).

d. *Tracking method WAM-2layers applied to EC-Earth data on pressure levels*

Originally, the WAM-2layers model was developed to perform moisture tracking with atmospheric data from

ERAI. We modify the WAM-2layers model in order to run it with input data from EC-Earth, which provides atmospheric data at five pressure levels, and to fit the purposes of this study. We describe the modifications below, whereas the results of the validation are presented in section 5b.

First, atmospheric data on pressure levels can intersect with topography. We use surface pressure to identify and eliminate levels which are situated below the surface. Thereafter, we perform a spline interpolation on the vertical flux profiles (uq and vq) at pressure levels to better estimate the real vertical wind profiles. A spline interpolation is chosen to better capture the LLJ. We perform a linear interpolation for the vertical profiles of specific humidity. Afterward, the interpolated data is integrated to two layers (bottom and top), which is needed for the tracking model (see previous section).

Second, we apply a linear interpolation of the moisture fluxes ($\partial F_x/\partial x$ and $\partial F_x/\partial y$) over time.

Third, when there is a local nonclosure of the moisture balance (i.e., on gridcell level) it can happen that the amount of water vapor in a cell S_k is smaller than the amount of tracked water vapor $S_{m,k}$. We allow this to happen, in order to ensure water conservation.

The spatial resolution of the EC-Earth data (~25 km × 25 km) is much higher than the spatial resolution of the ERAI data (~150 km × 150 km) and therefore we decrease the time step of WAM-2layers from 15 to 6 min. All simulations are performed on the following domain: 150°–50°W and 10°–70°N (Fig. 1).

e. Experimental setup

Here we describe the analyses in the same order as we discuss the results. First, we compare monthly basin averages of daily evaporation and precipitation from EC-Earth with CMIP5 model simulations, reanalyses, and observations. We indicate the interannual variance per model by showing the standard deviation of the monthly means per month, where we take the average of the standard deviations over all models for the CMIP5 ensemble. Variance between models, for the CMIP5 ensemble, is determined as standard deviation between each year for the different models and then averaging over the years.

Second, we quantify the spatial changes of E, relative humidity (RH), and P toward the future over Northern America. We determine if the change is statistically significant by bootstrapping the monthly averages per season (3 months per season × 30 years) to a sample of 1000. Then we calculate the 95% confidence intervals. If there is no overlap between the confidence intervals of the present and future variable, the change is deemed significant.

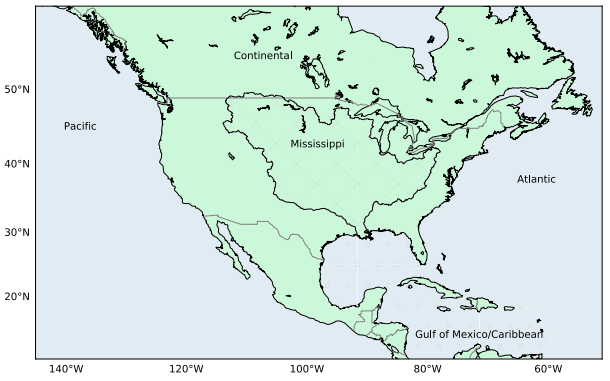

FIG. 1. Map of the domain on which we performed the moisture tracking, including the source regions used for analyses: continental area outside Mississippi River basin (green, not hatched), Mississippi River basin (green, hatched), Pacific (blue left of the continent), Atlantic (blue right of the continent, including Hudson Bay), and Gulf of Mexico/Caribbean (blue dotted).

Thereafter, we validate the closure of the water balance in the EC-Earth data (section 5a). In addition, we validate the changes made in the WAM-2layers model by running the adapted version with ERAI at the pressure levels which are available in the EC-Earth model (surface pressure, 850, 700, 500, 300, and 200 hPa), and we compare these results with the simulations from the original WAM-2layers code with ERAI at model levels. This validation is done for the year 2002.

We analyze the moisture sources per season (DJF, MAM, JJA, SON), for present climate (pr), future climate (fu), and the difference (Δ fu − pr). We determine the statistical significant differences in absolute moisture sources per season using bootstrapping and 95% confidence intervals (as described before). For further quantification, we determine the contribution of moisture source per geographical region. These regions are defined as follows: Mississippi River basin itself, continental areas outside the basin, Pacific Ocean, Gulf of Mexico/Caribbean, and the Atlantic Ocean (see Fig. 1). To allow a fair comparison between present and future moisture sources, the sources are normalized with the area-averaged precipitation falling over the MRB in the respective period. We indicate the robustness of the relative sources with error bars, which show the 95% confidence intervals after bootstrapping 1000 realizations (Efron and Tibshirani 1994) of the monthly average sources over the regions. To support the results, we include an extra analysis where we perform forward tracking to determine the moisture sinks (precipitation) from a selected source region (evaporation over the

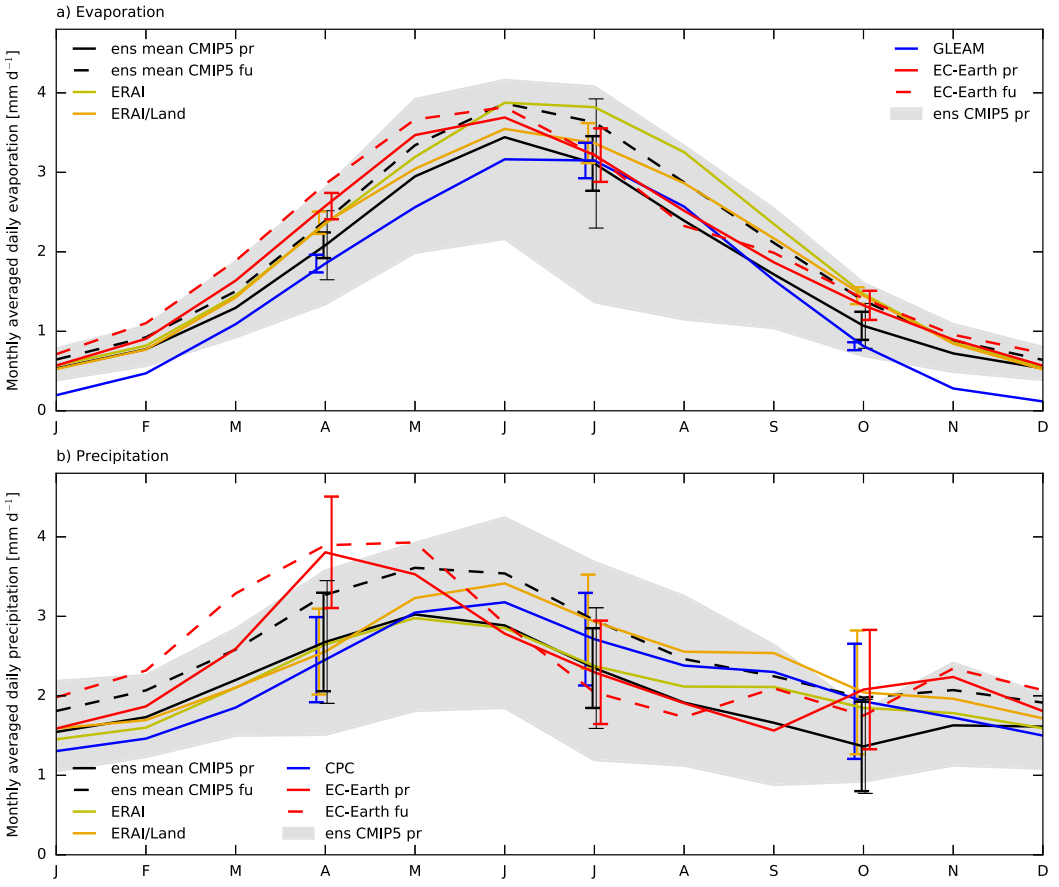

FIG. 2. Monthly averages of (a) basin-averaged daily evaporation (mm day^{-1}) and (b) basin-averaged daily precipitation (mm day^{-1}) over the MRB. The gray shading denotes the AMIP CMP5 1979–2008 coverage of model means around the ensemble mean (black line). Additional plotted data includes ensemble mean from CMIP5 future RCP4.5 (2070–2100; black dashed), CPC 1985–2014 precipitation and GLEAM 1985–2014 evaporation (blue), ERA-Interim 1985–2014 (yellow), ERA-Interim LAND 1985–2010 (brown), and EC-Earth present (6 × 2002–06; red solid line) and future climate (6 × 2094–98; red dashed line). The error bars indicate the standard deviation between the monthly values (interannual variance), in the corresponding color. We only show the error bars for the present day datasets (observations, EC-Earth pr, AMIP CMIP5 pr, and ERAI/Land) for the months April, July and October. The variance around ERAI is comparable to ERAI/Land and not shown. The thin black error bar around the ensemble mean of AMIP CMIP5 present indicates the standard deviation in the model spread.

southern Great Plains and northeast Mexico). These results are discussed in section 6b.

4. Evaporation and precipitation in present and future climate

a. Comparison of EC-Earth with CMIP5 model results and observations

We first compare monthly basin averages of daily evaporation and precipitation from EC-Earth with other model results (CMIP5 model means and ensemble mean), reanalyses, and observational data (Fig. 2). For evaporation, we find a pronounced yearly cycle with the smallest rates (~0.5 mm day^{-1}) and interannual variances in winter and largest rates (~3 mm day^{-1}) and interannual variances in summer. The variability among the CMIP5 models (black thin error bars) is largest in summer, when absolute values are largest. We find higher evaporation values in October–May in EC-Earth compared to most other CMIP5 models, the CMIP5 ensemble mean, and observations. For all months (shown for April, July, and October), the spread because of interannual variability in EC-Earth falls within the possibilities of CMIP5 output given by the model means (gray dotted lines).

In a future climate, we find increased values of evaporation in winter and spring (around 0.2 mm day^{-1}) using EC-Earth. Increased evaporation rates in spring and summer are found by comparing the ensemble mean of historical AMIP CMIP5 simulations with the ensemble

mean of future (RCP4.5) AMIP CMIP5 simulations. Ferguson et al. (2018) performed a similar analysis using the coupled runs from CMIP5 and the future simulations based on the RCP8.5 scenario, and found significant increases for evaporation in every month of the year except for July and August.

Furthermore, we compared the spatial pattern of evaporation simulated by EC-Earth over the whole domain with the reanalysis product ERA-Interim (the GLEAM product only provides evaporation over land and is therefore not useful to do a spatial comparison). Over land, EC-Earth and ERAI are very comparable, with a similar spatial distribution (not shown). Over the ocean, evaporation in EC-Earth is higher over the Gulf of California, Gulf of Mexico, and the Gulf Stream. It should be noted that EC-Earth has fixed SSTs and only simulates from 2002 to 2006, which makes the comparison nontrivial.

Within all models, we find high daily precipitation values in the beginning of summer, which is mainly related to convective precipitation, and lower values of daily precipitation in winter (Fig. 2b). There is a large variability in precipitation within the model means of CMIP5, in summer ranging from 1.5 to 4 mm day^{-1} (gray area). Precipitation simulated by EC-Earth falls mostly within this spread of model means, except for April and October. We find the peak in precipitation in May and June for CMIP5, CPC, and ERAI-Land whereas precipitation from EC-Earth peaks in April and May, falling outside the variability. However, the interannual variance from EC-Earth always overlaps with the interannual variance and model variance around the CMIP5 ensemble mean. The higher values for precipitation in winter and spring in EC-Earth compared to most other models were also found for evaporation. The model mean precipitation of the EC-Earth AMIP CMIP5 runs shows a similar pattern in precipitation, and evaporation, as the high-resolution simulations used in this study (not shown).

In a future climate with EC-Earth, higher precipitation amounts over the Mississippi are simulated in winter and spring (an increase of around ~0.5 mm day^{-1}). In July and August a decrease in precipitation over the basin is found toward the future. Precipitation from the ensemble mean of the CMIP5 future simulations is in every month higher than the ensemble mean from CMIP5 for the present (Fig. 2b). The study by Ferguson et al. (2018) found a significant increase in precipitation over the Mississippi basin from November to May using the coupled runs from CMIP5 and the RCP8.5 scenario for future simulations.

Despite the biases in precipitation in EC-Earth, the changes toward the future still contain valuable information, as studies show that there is a weak or nonexistent relation between obvious metrics of observable quantities and projections (Knutti et al. 2010). In the next section, we will focus on the spatial changes of components of the atmospheric water balance toward the future.

b. *Spatial changes in evaporation and precipitation in EC-Earth*

In simulations of future climate with EC-Earth (2094–98; RCP4.5) we find an increase in 2-m temperature of 2.5°–3°C over the ocean, and 3°–4°C over land, with the largest increases in the northern parts of the domain (not shown). Because of these higher temperatures, and an increase in evaporation in general, larger amounts of column integrated water vapor S are found over the whole domain and again especially in the northern parts.

We show the spatial distribution of the change in evaporation, relative humidity and precipitation toward the future for winter (DJF) and summer (JJA) in Fig. 3. Over the oceans, a general increase in evaporation is projected for the future, with locally increases up to 50 mm month^{-1}, for example over the Gulf Stream. Especially in winter (DJF) and autumn (SON, not shown) evaporation also increases over the southern parts of the domain, including the Gulf of Mexico (Fig. 3a). This increase in evaporation over the ocean is the result of an increase in saturated vapor pressure, which is driven by an increase in SST, and a relative humidity that significantly but unsubstantially changes toward the future (0%–2%, Fig. 3b).

In contrast to oceans that provide an infinite source of water to evaporate, land evaporation is limited by soil moisture and a rise in temperature does not automatically imply an increase in evaporation. We find that soil moisture availability limits evaporation in winter, as the change in evaporation and relative humidity are spatially correlated, both positive in the north and both negative in the southwest (Figs. 3a,b). In the north (over the MRB), an increase in evaporation combined with an enhancement in relative humidity points to an increase in the supply of water (van Heerwaarden et al. 2010), thus an increase in soil moisture. In the southwest, a decrease in evaporation leads to an increase in sensible heat flux, which heats up the boundary layer and which decreases the relative humidity. It should be noted that other aspects like frozen ground, snow cover, and vegetative seasonality can also influence the relation between soil moisture and evaporation in winter, but are not assessed in this study. The same signal with decreased evaporation rates and decreased relative humidity is found in spring and summer over Mexico (Figs. 3d,e). This decrease in evaporation toward the

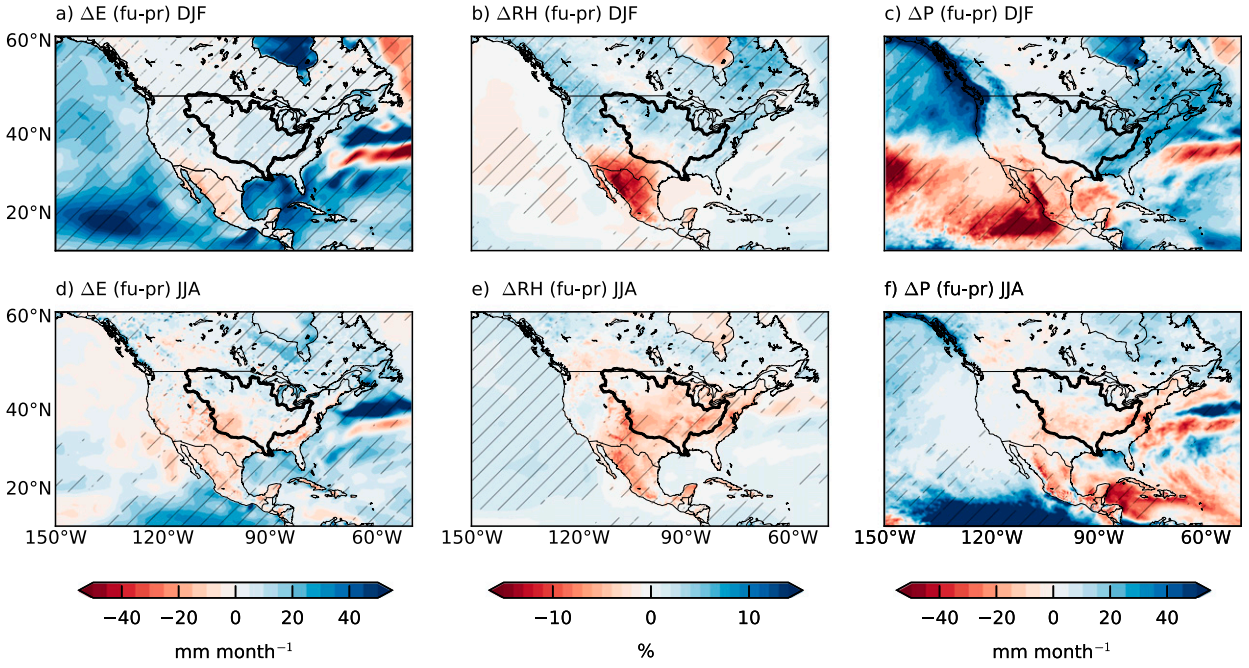

FIG. 3. Spatial patterns of the change in EC-Earth RCP4.5 (a),(d) evaporation ΔE (future − present; mm month^{-1}), (b),(e) relative humidity ΔRH (future − present; %), and (c),(f) precipitation ΔP (future − present; mm month^{-1}) for (top) DJF and (bottom) JJA. Significant differences are indicated with hatching.

future is also found by Seager et al. (2007), using a large suite of climate models.

In summer (JJA) over the MRB, except for the northwestern corner, an increase in evaporation corresponds with a decrease in relative humidity. Here, soil moisture may not be the limiting factor and the increase in evaporation could be mainly related to an increase in temperature (highest increases of temperature were also found in the northern parts). If increases in temperature dominate over increases in humidity, relative humidity will decrease (Fig. 3e).

For precipitation, we find an increase in winter and spring over the MRB (Figs. 3c and 2b), especially in the central and eastern part of the basin. The strongest increase in precipitation in winter outside the MRB occurs along the northwest coast and the strongest decrease outside the MRB over the South Pacific and southeastern North America and Mexico. In summer, we find a slight decrease in precipitation over the MRB (Figs. 2b and 3f). The most obvious positive change in summer (JJA) is found over the tropical Pacific with much higher precipitation rates in future, while over the Caribbean a negative change of precipitation to the future is found.

Additionally, we also find a clear dipole of positive and negative changes in E and P over the North Atlantic Ocean. This has been attributed to a too far north location of the Gulf Stream in the ECHAM5/MPI-OM model (Sterl et al. 2008), which is used to determine the SST projections of the EC-Earth future simulations. Furthermore, the changes in circulation (wind) over North America to the future are very small (not shown), except for JJA where we find a strengthening of the circulation over central North America, which is discussed further in section 6b.

5. Validation of WAM-2layers with input data from EC-Earth

a. *Closure of atmospheric water balance in EC-Earth*

We first assess the closure of the atmospheric water balance within the EC-Earth data. We find that over the whole domain, and over the time period of one year (2002) the atmospheric water budget closes almost totally (−0.06%). However, per time step (6-hourly) the local nonclosure of the balance per grid cell can be substantial (up to 20 mm day^{-1}). The largest nonclosure occurs mostly under large gradients of specific humidity. The nonclosure can occur because we use instantaneous 6-hourly atmospheric data (wind and specific humidity), and because we have a coarse representation of the lowest layer of the atmosphere where the highest amounts of moisture occur (between surface pressure and 850 hPa). Furthermore, we do not use the same numerical methods for discretization as were used in the spectral EC-Earth model. Finally, the fact that atmospheric data is transformed from model levels to

TABLE 1. Relative contribution of moisture sources per region contributing to precipitation over the MRB (%) averaged for the year 2002. The column with ERAI model levels indicates the results with the standard version of WAM-2layers and ERA-Interim at model levels. The column with ERA-Interim five pressure levels shows the results with the adapted version of WAM-2layers with ERA-Interim data at five pressure levels.

Relative source (%)		ERA-Interim model levels 2002	ERA-Interim five pressure levels 2002
Nonclosure in WAM-2layers		100 − 99.6 = 0.4	100 − 99.5 = 0.5
Tracked source	Total	73.4	71.7
	Mississippi River basin	12.6	12.4
	Continental (not Mississippi)	18.9	19.0
	Atlantic	8.5	7.0
	Gulf of Mexico/Caribbean	15.6	14.9
	Pacific	17.8	18.2
Outflux over boundaries	East	6.7	6.2
	West	14.1	14.5
	North	0.6	0.3
	South	5.7	7.9

pressure levels also contributes to the nonclosure of the water balance (Trenberth 1991; Seager et al. 2010; Seager and Henderson 2013). Nevertheless, the nonclosure at the local gridcell level does not lead to a nonclosure of the water balance over the whole domain in 2002 in the EC-Earth data.

We do not assess the (local non-)closure of the atmospheric water budget in ERAI, but expect similar results as for EC-Earth as both models are based on the same numerical weather prediction model (IFS). ERAI does provide atmospheric variables close to the surface, however due to data assimilation other biases may be introduced (Trenberth et al. 2011).

b. Validation to apply WAM-2layers with EC-Earth

We run the adapted version of the WAM-2layers model with ERAI at the pressure levels that are available in the EC-Earth model, and we compare these results with the simulations from the original WAM-2layers code with ERAI at model levels (Table 1).

The first row of Table 1 indicates the nonclosure of the water balance with the WAM-2layers model (i.e., how much water is lost between source and sink), when run with ERAI at model levels (first column) and run with ERAI at five pressure levels (second column). This term is related to the nonclosure of the water balance per grid cell as discussed in section 5a.

Table 1 quantifies the contributions per source region in percentage. We find very small differences in using model levels versus five pressure levels between sources from continental areas (Mississippi River basin and surrounding continental areas) and the Pacific. For the Atlantic and Gulf of Mexico and Caribbean the differences are slightly larger. By using the data at pressure levels we lack information in the lowest layer which leads to an underestimation of the velocities associated with the LLJ, which is an important mechanism in the warm season to transport moisture from these regions toward the MRB.

Note that we do not perform the tracking globally, to reduce computational costs, and therefore some tracked moisture crosses the boundaries of the domain. This is indicated in Table 1 with the outfluxes over the boundaries (east, west, north, and south). We find the largest outflux at the western boundary.

From this validation we conclude that the moisture sources of the MRB determined with ERAI at model levels and ERAI at five pressure levels are comparable, thus that we can apply WAM-2layers to the available data from EC-Earth.

6. Moisture sources and recycling ratios of the Mississippi River basin in present and future climate

a. Seasonal variability of the moisture sources in present climate in EC-Earth

We show the moisture sources E_m of the MRB in present climate averaged per season in Fig. 4 (left column). The amount of precipitation occurring over the river basin is indicated in the titles. We find that the most important continental moisture sources are the MRB itself and the continental area southwest of the basin. The most important oceanic sources are the Gulf of Mexico and Caribbean and the (South) Atlantic and (east) Pacific. In the (east) Pacific Ocean, the sources are mainly found around the Gulf of California.

There is a large seasonal variation in the moisture sources. In winter (DJF), the moisture sources are mostly located over the oceans, because evaporation over the oceans is much larger than over land during winter. Moisture is transported with the westerlies from the Pacific toward the MRB, and with an anticyclonic

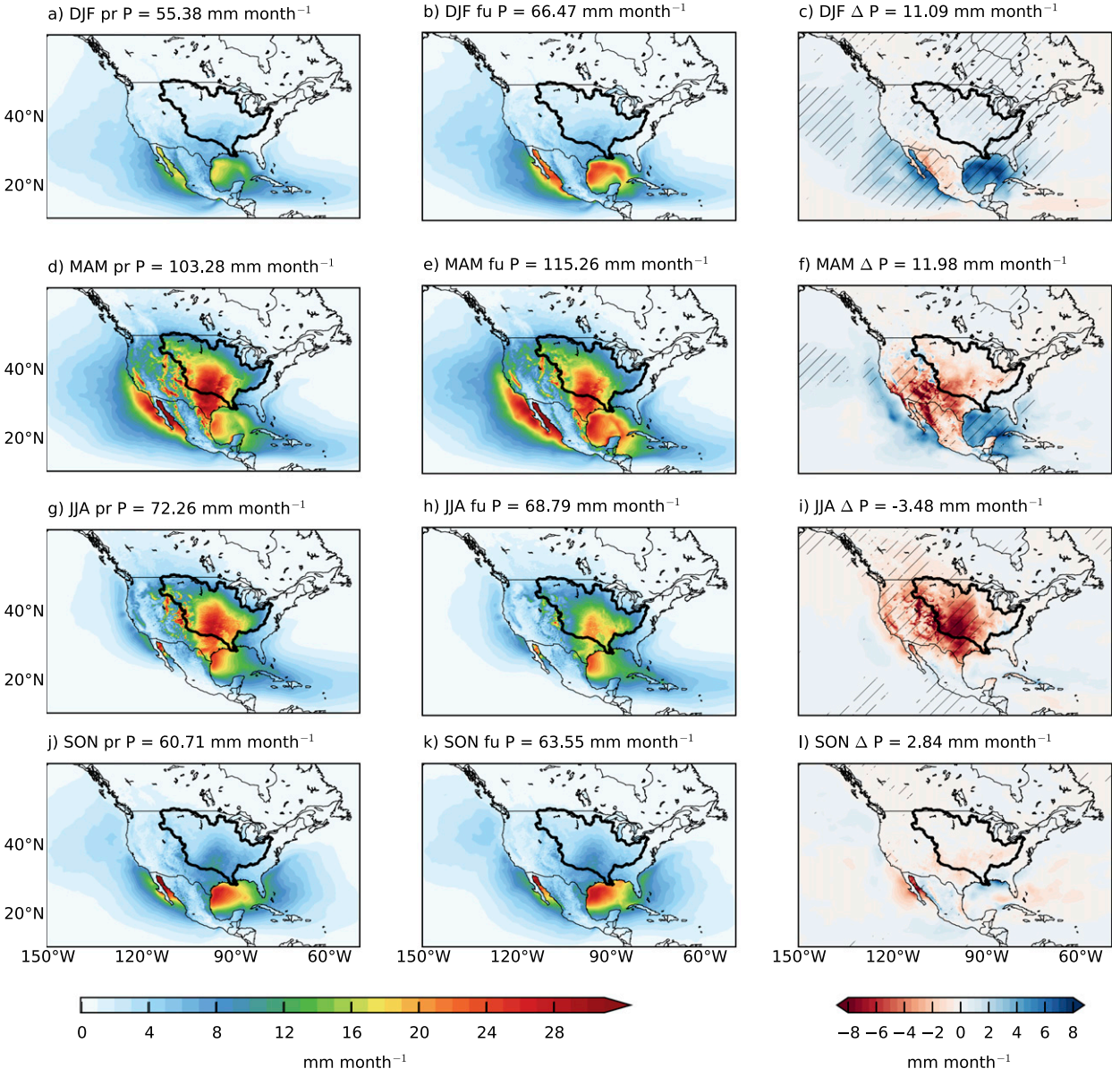

FIG. 4. The absolute moisture sources E_m of precipitation over the Mississippi River basin (basin indicated with thick black line) in present and future climate for (a)–(c) DJF, (d)–(f) MAM, (g)–(i) JJA and (j)–(l) SON (mm month^{-1}) from EC-Earth. The sources for (left) present climate (pr), (center) future climate (fu), and (right) the difference (Δ) fu − pr. The statistically significant differences are indicated with hatching in the (Δ) fu − pr plots. The monthly averaged precipitation over the MRB is indicated in the subplot titles.

flow (Bermuda high) and LLJ from the Atlantic and Gulf of Mexico and Caribbean toward the MRB. In spring (MAM), the moisture sources over land increase as the increasing solar radiation drives the evaporation. This increase in sources over land, together with supply of moisture from the oceans, results in high precipitation amounts in spring over the MRB (~100 mm month^{-1}), although spring precipitation is overestimated in EC-Earth compared to observations and other simulations (Fig. 2b). In the summer (JJA), the Pacific (Gulf of California) moisture sources substantially decrease, resulting in less precipitation over the MRB. The source contribution from the Gulf of Mexico is similar in MAM as in JJA. During this warm season, the Bermuda high is shifted westward enhancing the Great Plains LLJ which results in large amounts of moisture being transported from the Gulf of Mexico as far as the northeast United States (Algarra et al. 2019).

Dirmeyer and Kinter (2010) studied the moisture sources of the Midwestern region of the United States during late spring and summer (May–July). The spatial distribution of moisture sources (Fig. 4 in Dirmeyer and Kinter 2010) is comparable to our study. However, their contribution of continental sources is larger, which could be caused by their study region which is smaller and located more land-inwards. Evaporation rates over land peak during summer and most precipitation in the MRB is convectively driven (Benedict et al. 2019), that is, moisture is recycled within the river basin. The evaporation recycling ratio as defined in Eq. (4) is around 20% in summer (compared to 10% in winter), which means that 20% of the evaporation occurring over the MRB results in precipitation within the same basin. In SON, sea surface temperatures are still high, resulting in high oceanic evaporation rates. However, land evaporation decreases compared to summer, and therefore the main source of moisture for precipitation over the MRB in SON is the Gulf of Mexico (Fig. 4j).

To summarize, we find that the moisture sources are varying throughout the seasons, with high recycling rates over land during MAM and JJA, and a dominant role of advection of moisture from the oceans to the MRB during SON.

b. *Moisture sources in a future climate*

The projected moisture sources of the MRB in a future climate are shown per season in Fig. 4 (center column) and the difference between present and future in the right column, where significant differences are indicated with hatching. The future seasonal spatial patterns of moisture sources are similar to the spatial patterns in present climate, but there are differences in the strength of the sources, especially in winter (DJF) and summer (JJA). Over the Gulf of Mexico and the Gulf of California, the moisture source is strongly increased in winter from maximum source values in present climate of 20 mm month^{-1} to values of 30 mm month^{-1} in a future climate (Fig. 4c). This is related to an increase in evaporation over the oceans in winter (Fig. 3a), and results in an increase in precipitation over the MRB in winter of 10 mm month^{-1}. In MAM, an increase in moisture source of 8 mm month^{-1} over the Gulf of Mexico is found, which can also be related to an increase in precipitation over the MRB. In summer (JJA), we find a decrease of moisture source over continental areas of around 10 mm month^{-1}, both within the MRB and south and west from the river basin. However, we do not find such a large decrease in evaporation in this period (Fig. 3b). In autumn (SON), there are no large differences in moisture source and precipitation between present and future climate.

If in a future climate more or less precipitation over the MRB occurs, more or less moisture will be tracked. Therefore, we normalize the absolute sources with precipitation over the MRB ($\int_A \delta E_m \, dA / \int_{dA} \delta P \, dA$) and show the relative contribution per region and season in Fig. 5, and the robustness with 95% confidence intervals obtained after bootstrapping (Efron and Tibshirani 1994) the monthly average sources over the regions. We also show the yearly averaged relative contribution of all land regions and all ocean regions, and thereby we include the yearly average relative moisture sources which leave the domain over the four boundaries (north, east, south, west).

Averaged over all seasons (Figs. 5f,g and numbers in Table 2), we find a significant decrease of relative moisture sources over land from 33% in present climate to 27% in a future climate. The relative contribution of oceanic moistures sources slightly increases from 44% to 47% (Fig. 5g). The rest of the moisture is transported out of the domain. If we focus on the different seasons (Fig. 5), we find that in DJF and MAM the relative moisture source contribution from the Gulf of Mexico and Gulf of California (Pacific) is slightly increased. These slight increases in moisture sources over the ocean lead to an increase in precipitation over the MRB. The contribution of terrestrial moisture sources over land is declined for all seasons. For the continental areas outside the MRB this decrease can be mostly attributed to MAM and JJA, and for a lesser extent to DJF. For the MRB the largest decline in relative moisture source is found in MAM and JJA.

A different way to show the contribution of sources over land (MRB) to precipitation over the MRB is the evaporation recycling ratio. Figure 6 shows the monthly-averaged evaporation recycling ratio, as defined in Eq. (4), for the present and future climate. This evaporation recycling ratio is not directly comparable to the recycled precipitation fractions mentioned in the Introduction, which are determined using forward moisture tracking. We find a lower yearly averaged evaporation recycling ratio in future (0.12) compared to present (0.14). For both periods, we find larger evaporation recycling ratios in summer compared to winter. In summer, land evaporation is highest and triggers local convective precipitation, and therefore recycling of moisture within the basin, while in winter relatively more moisture is advected into the MRB. In the simulations of future climate, we find that the evaporation recycling ratios are significantly lower in April–July and October compared to present conditions, consistent with our previous results (Fig. 5).

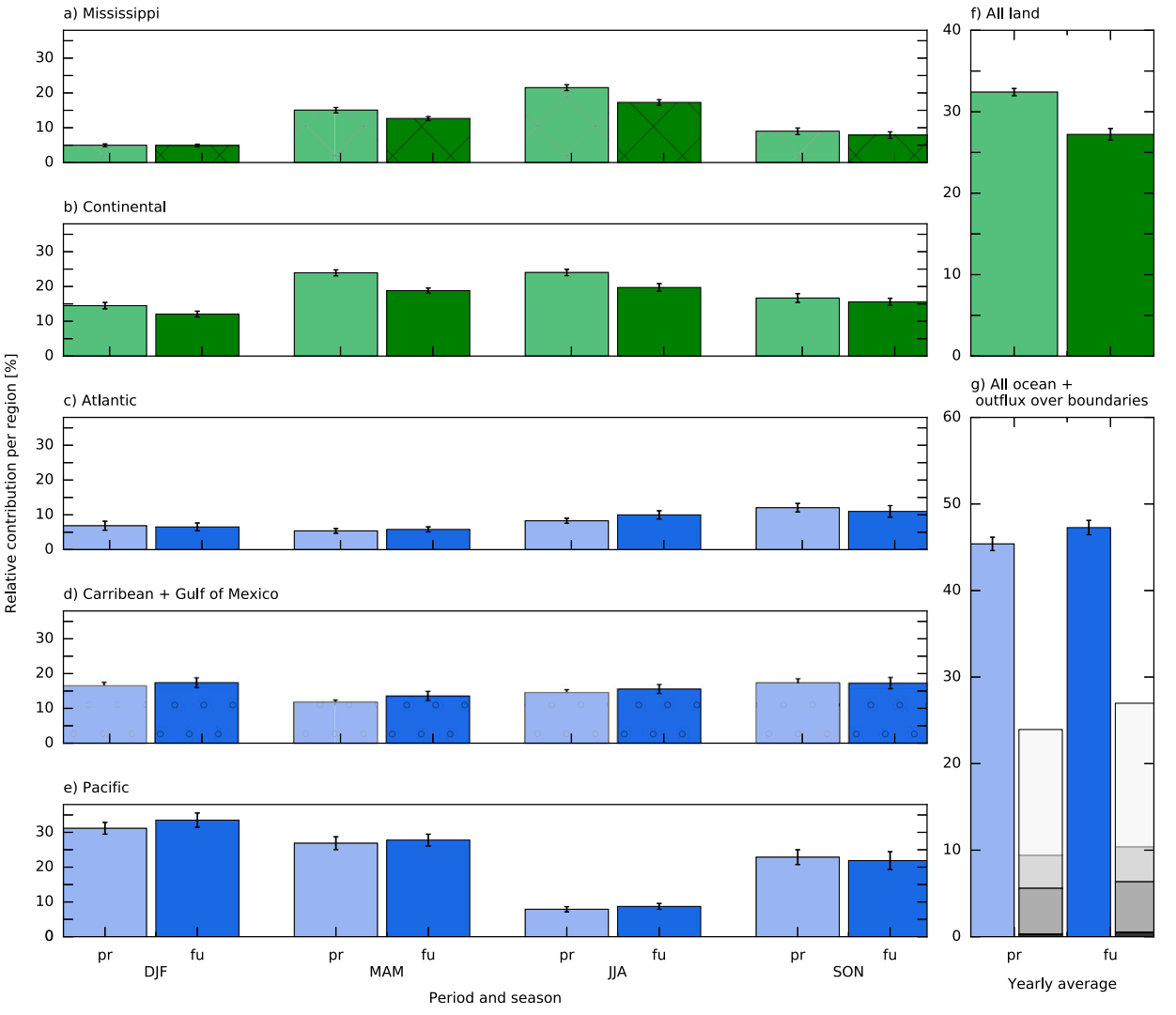

FIG. 5. (a)–(e) Relative contribution of moisture sources per region contributing to precipitation over the MRB ($\int_A \delta E_m \, dA / \int_{dA} \delta P \, dA$). Seasonal MRB precipitation totals are included as subplot titles in Fig. 4. The moisture source contribution per region is shown for each season (DJF, MAM, JJA, and SON) for present and future climate from EC-Earth. The area covering the Gulf of Mexico and Caribbean is indicated in Fig. 1. We also show the yearly average relative contribution for (f) all land and (g) all oceans and the fluxes over the boundaries of the domain for north–east–south–west from the black to white colors. These numbers are also presented in Table 2. The error bars indicate the 95% confidence intervals after bootstrapping the monthly averages.

There are two hypotheses that can explain the decrease in (relative) terrestrial moisture source over land. Either there is less moisture to evaporate over land (drier soils in a future climate), or the evaporated water rains out downstream of the MRB. For the first hypothesis, we expect less evaporation in a future climate in the months (JJA) where the moisture source over land has decreased. We do find a decrease in evaporation in JJA over the MRB (a decrease of 0.92 mm month^{-1} averaged over the basin), but this decrease is smaller than the decrease in moisture source over the MRB (3.39 mm month^{-1}). Therefore, the decrease in evaporation cannot explain the decrease in moisture source.

To evaluate the second hypothesis, we use forward tracking to determine the precipitation sinks related to the land region where we find a decrease in JJA moisture source (southwest MRB and southwest of the MRB, see Fig. 4i). We performed forward tracking from May to September, as these are the months during which we find the (largest) decrease in moisture source from land. Figure 7 shows the precipitation sinks, for both present and future climate, and the difference between future and present. We find a decrease in tracked

TABLE 2. Relative contribution of moisture sources per region contributing to precipitation over the MRB (%) from EC-Earth averaged over 30 years (6 members from 2002 to 2006 for present climate and 6 members from 2094 to 2098 for future climate).

Relative source (%)		EC-Earth present 6 × 2002–06	EC-Earth future 6 × 2094–98
Terrestrial	Mississippi River basin	13.2	10.9
	Continental (not Mississippi)	20.0	16.4
Oceanic	Atlantic	8.1	8.1
	Gulf of Mexico/Caribbean	14.5	15.5
	Pacific	21.6	23.1
Outflux over boundaries	East	5.2	5.6
	West	13.4	15.9
	North	0.3	0.4
	South	3.6	3.8

precipitation south of 40°N, which was also found in the spatial changes of precipitation in Fig. 3d. We also find a small increase in tracked precipitation in the north within the MRB and north of the river basin, and also in the region of Florida (Fig. 7f). This can be related to an increase in the moisture fluxes over mid North America in the future (integrated moisture fluxes indicated with arrows in Figs. 7d–f). We also find an increase in southerly winds at 10 m and at 850 hPa in the same area in the future (not shown), indicating a strengthening of the circulation in the summer. The Great Plains LLJ is the most important moisture transport mechanism in summer in mid North America, and previous studies reported a strengthening of the Great Plains LLJ because of a westward shift of the Bermuda high in April–June in the future (Cook et al. 2008; Seager et al. 2014). To summarize, our second hypothesis is confirmed as we find that more moisture is transported out of the river basin in the future.

7. Discussion on methodology

We used the Eulerian water tracking model WAM-2layers (van der Ent et al. 2010, 2014) to determine the moisture sources of the MRB. There are also other approaches to determine the moisture sources of a region, such as online water vapor tracers (Knoche and Kunstmann 2013; Singh et al. 2016) and Lagrangian tracking (Stohl and James 2005; Sodemann et al. 2008; Dirmeyer and Brubaker 2007). Online tracking will provide the most realistic moisture sources as the tracking is performed on full model resolution, but it is computationally very expensive and backward tracking is impossible. The performance of offline Lagrangian tracking depends on the amount of parcels that are tracked, which relates to the computational expense of the tracking, with longer time series being computationally more expensive. This is also the case for Eulerian tracking. In the study by van der Ent et al. (2013) the three approaches mentioned were compared for moisture recycling over the Volta region (West Africa). They found only one percent difference in recycling ratio determined with the online method and the WAM-2layers method with ERA-Interim data (Table 2 in van der Ent et al. 2013). We show here that WAM-2layers can also be applied to global climate simulations with higher horizontal resolution, but less information in the vertical, compared to ERA-Interim (Table 1). By performing a spline interpolation on the moisture fluxes we found an overall better representation of the seasonally varying Great Plains LLJ. We conclude that an Eulerian approach is an appropriate method to perform moisture tracking for climate simulations, over longer time periods (2 × 30 years), and over a large region (North America) using high-resolution data. Nevertheless, a comparison of moisture sources determined with different datasets and tracking approaches is recommended, for example such as done by Hoyos et al. (2018).

The horizontal resolution of the data used here is ~25 km, and there are only a few climate models that

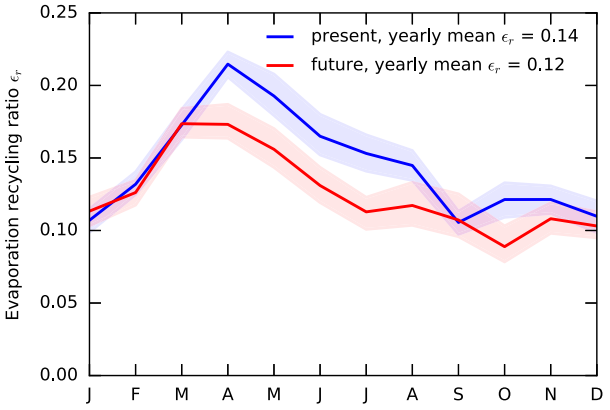

FIG. 6. The monthly averaged evaporation recycling ratio $\epsilon_r = \int_A \delta E_m \, dA / \int_A \delta E \, dA$ for the Mississippi River basin in present and future conditions according to EC-Earth. The shaded bands indicate the 95% confidence intervals after bootstrapping the monthly average ratios.

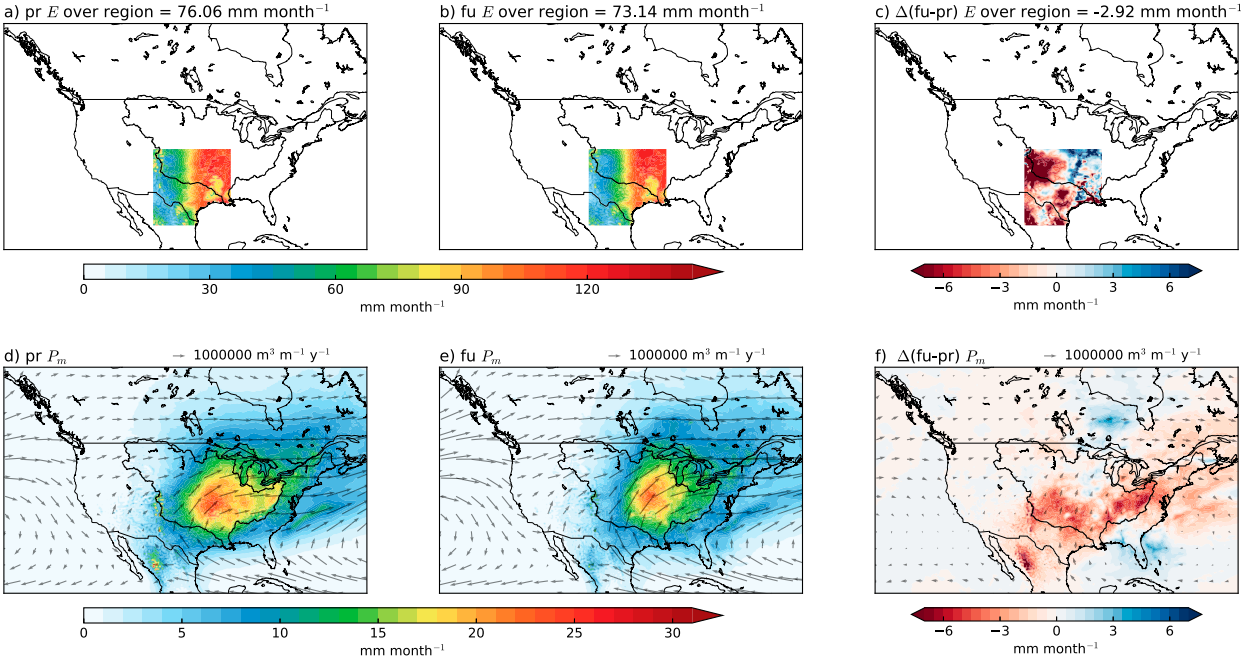

FIG. 7. (top) Forward tracking of the May–September evaporation over the tracked subdomain (107°–95°W, 25°–40°N, land only) for (a) present, (b) future, and (c) Δ fu − pr. The monthly area-averaged evaporation over the tracked domain is indicated in the titles (mm month^{-1}). (bottom) Shown in shading is the tracked precipitation P_m and in arrows the moisture fluxes for (d) present, (e) future, and (f) Δ fu − pr. The arrows indicate the integrated moisture fluxes over the whole atmosphere.

have run simulations for both present and future climate at such a high spatial resolution, and for a time period of 30 years (Murakami et al. 2015). However, for present climate only, studies have been performed at such high resolution to assess the atmospheric water transport, however without moisture tracking. Demory et al. (2014) found an increase in transport of water from oceans to land with higher spatial resolution simulations (from 135 to 25 km and from 270 to 60 km), as more precipitation will occur over land than over the ocean, indicating that the partitioning of moisture sources changes from local to more nonlocal moisture sources. Nevertheless, in spectral models such as EC-Earth, it was found that the moisture advection to land increases less with resolution (Vannière et al. 2019). We use similar high resolution simulations as the study from Demory et al. (2014) and Vannière et al. (2019) but expand the sensitivity of the moisture sources toward the future for the MRB, concluding that moisture sources over the ocean increase and moisture sources over land decrease. This indicates that both increased spatial resolution, as well as future projections, will lead to an increase in moisture transport from oceans to land, affecting the water resources of river basins. Findell et al. (2019) performed moisture tracking on low resolution earth system model simulations of historical and future climate and found also an increase in oceanic sources resulting in continental precipitation. The robustness of this increase in oceanic sources can be assessed when more high-resolution simulations for future climate are available, for example within the Horizon 2020 project PRIMAVERA (https://www.primavera-h2020.eu/) and the CMIP6-endorsed HighResMIP (Haarsma et al. 2016).

The results presented in this study are based on one model and 30 years of simulations for both present and future climate. Due to this finite length we do not study multidecadal variabilities, but focus instead on the mean change in moisture sources under climate change.

The EC-Earth model is constrained with sea surface temperature, limiting the variability of the simulations. While we capture some interannual variability (6×5 years), we do not analyze this in detail. From previous studies we know that the moisture sources and/or regional recycling can differ substantially from year to year (Dirmeyer and Brubaker 1999; Bosilovich and Schubert 2001), and that multidecadal and interdecadal (such as El Niño) variability can produce large variations in the precipitation over the MRB. It would be of interest to further study the variability in moisture sources in combination with these large-scale interannual variations, to better predict and project the moisture sources of the Mississippi. However to do so, longer simulations and more ensembles are needed,

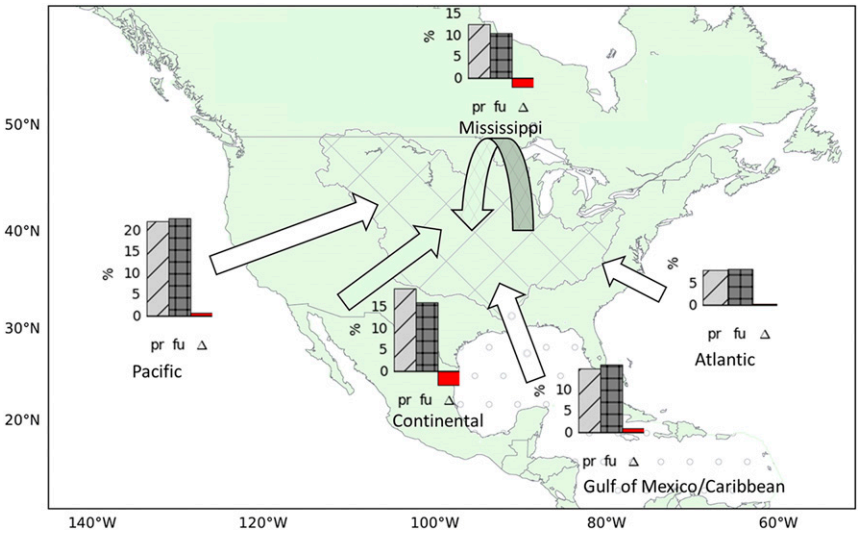

FIG. 8. Mean annual moisture transport to the MRB indicated with arrows (drawn to scale). The arrow indicates if the origin is oceanic (white) or continental (green). The bar plots indicate the relative contribution of evaporation to precipitation over the MRB for present (pr), future (fu), and the difference between present and future (Δ fu − pr). The numbers in these figures are also given in Table 2. The differences between present and future are significant for the terrestrial sources, but not significant for the oceanic sources.

which are currently unavailable at the spatial resolution of our dataset. Simulations covering a longer time period can also be used to understand moisture sources under extreme or compound events (such as compound fluvial and coastal flooding), and especially how these sources of extreme events are affected by climate change. Last, although this study focuses on the moisture sources of the MRB, the methodology used in this study can also be applied to other regions of interest.

8. Summary and conclusions

We study the changes in the moisture sources, resulting in precipitation over the Mississippi River basin, under climate change. To do so, we make use of a set of high spatial resolution (~25 km) simulations of 30-yr present and 30-yr future climate from EC-Earth. We use the output of one climate model and only focus on the mean change toward the future.

We first validate precipitation and evaporation from EC-Earth with model simulations and observations. Evaporation from EC-Earth falls within the variability of CMIP5 model mean simulations, where precipitation from EC-Earth is positively biased in spring. Second, we study the local spatial changes of evaporation, relative humidity and precipitation over North America under climate change (Fig. 3). Evaporation is increasing over large parts of the domain, and especially over the southern part of the oceans. This increase is related to an increase in SST and an almost constant relative humidity. In summer, we find a decrease in evaporation over southwest North America, probably because of drier soils. This also results in lower relative humidity and less precipitation in this region. Precipitation over the MRB increases toward the future in winter and decreases in summer (Figs. 2 and 3).

Third, we determine the moisture sources of the MRB under present and future climate conditions using an adapted version of the Eulerian WAM-2layers tracking model which fits the EC-Earth climate simulations, and which was validated using ERA-Interim reanalysis data (Table 1). Averaged over the 30 years of present climate, we find a contribution of moisture sources from continental (land) origin of 33% and from oceanic origin of 44%, where the rest is transported out of the domain. The most important continental moisture sources are the sources within the MRB itself and the continental area southwest of the basin. The most important oceanic sources are the Pacific and Gulf of Mexico and Caribbean (Figs. 4 and 8). The sources are seasonally varying, with more recycling of moisture within the river basin in summer and more transport of moisture from the ocean toward the MRB in winter. In the future, the moisture source contribution from oceanic origin increases from 44% to 47%, and the contribution from continental origin decreases from 33% to 27%. The increase in moisture source from the ocean is small

and mainly found in winter (higher SST leads to higher evaporation rates), especially over the Gulf of Mexico, and results in more precipitation over the MRB in winter (Fig. 4). In summer, we find a significant decrease in moisture sources from the basin itself (i.e., lower recycling ratios within the basin, Fig. 6) and from the continental areas outside the basin (Fig. 8), although precipitation is not decreasing. We find that higher moisture fluxes over mid North America in the future result in a larger transport of moisture outside of the basin.

We conclude that the moisture sources of the Mississippi River basin in the future 1) enhance over the oceans in winter, resulting in more future winter precipitation, and 2) show a relative decline over terrestrial areas in summer, indicating that land surface properties will have relatively less impact on precipitation over the Mississippi River basin in the future.

Acknowledgments. We would like to acknowledge ECMWF for supplying ERA-Interim data through their server at http://www.ecmwf.int. The EC-Earth data are available upon request by the author. The original WAM-2layers code is available on Github (https://github.com/ruudvdent/WAM2layersPython), as well as the adapted version used in this study (https://github.com/Imme1992/moisture_tracking_mississippi). The simulations are performed on the Cartesius supercomputer from SURFsara (project number SH-312-15). Imme Benedict and Ruud van der Ent both acknowledge funding from the Netherlands Organization for Scientific Research (NWO) for projects 869.15.004 and 016.Veni.181.015, respectively.

REFERENCES

Algarra, I., J. Eiras-Barca, G. Miguez-Macho, R. Nieto, and L. Gimeno, 2019: On the assessment of the moisture transport by the great plains low-level jet. *Earth Syst. Dyn.*, **10**, 107–119, https://doi.org/10.5194/esd-10-107-2019.

Allen, M. R., and W. J. Ingram, 2002: Constraints on future changes in climate and the hydrologic cycle. *Nature*, **419**, 228–232, https://doi.org/10.1038/nature01092.

Baatsen, M., R. J. Haarsma, A. J. van Delden, and H. de Vries, 2015: Severe autumn storms in future western Europe with a warmer Atlantic Ocean. *Climate Dyn.*, **45**, 949–964, https://doi.org/10.1007/s00382-014-2329-8.

Balsamo, G., A. Beljaars, K. Scipal, P. Viterbo, B. van den Hurk, M. Hirschi, and A. K. Betts, 2009: A revised hydrology for the ecmwf model: Verification from field site to terrestrial water storage and impact in the integrated forecast system. *J. Hydrometeor.*, **10**, 623–643, https://doi.org/10.1175/2008JHM1068.1.

——, and Coauthors, 2013: ERA-Interim/Land: A global land water resources dataset. *Hydrol. Earth Syst. Sci.*, **19**, 389–407, https://doi.org/10.5194/hess-19-389-2015.

Benedict, I., C. C. van Heerwaarden, A. H. Weerts, and W. Hazeleger, 2019: The benefits of spatial resolution increase in global simulations of the hydrological cycle evaluated for the Rhine and Mississippi basins. *Hydrol. Earth Syst. Sci.*, **23**, 1779–1800, https://doi.org/10.5194/hess-23-1779-2019.

Benton, G. S., R. T. Blackburn, and V. O. Snead, 1950: The role of the atmosphere in the hydrologic cycle. *Eos, Trans. Amer. Geophys. Union*, **31**, 61–73, https://doi.org/10.1029/TR031i001p00061.

Bosilovich, M. G., and S. D. Schubert, 2001: Precipitation recycling over the central united states diagnosed from the geos-1 data assimilation system. *J. Hydrometeor.*, **2**, 26–35, https://doi.org/10.1175/1525-7541(2001)002<0026:PROTCU>2.0.CO;2.

——, and ——, 2002: Water vapor tracers as diagnostics of the regional hydrologic cycle. *J. Hydrometeor.*, **3**, 149–165, https://doi.org/10.1175/1525-7541(2002)003<0149:WVTADO>2.0.CO;2.

——, and J.-D. Chern, 2006: Simulation of water sources and precipitation recycling for the Mackenzie, Mississippi, and Amazon River basins. *J. Hydrometeor.*, **7**, 312–329, https://doi.org/10.1175/JHM501.1.

Brubaker, K. L., D. Entekhabi, and P. Eagleson, 1993: Estimation of continental precipitation recycling. *J. Climate*, **6**, 1077–1089, https://doi.org/10.1175/1520-0442(1993)006<1077:EOCPR>2.0.CO;2.

——, P. A. Dirmeyer, A. Sudradjat, B. S. Levy, and F. Bernal, 2001: A 36-yr climatological description of the evaporative sources of warm-season precipitation in the Mississippi River basin. *J. Hydrometeor.*, **2**, 537–557, https://doi.org/10.1175/1525-7541(2001)002<0537:AYCDOT>2.0.CO;2.

Cook, K. H., E. K. Vizy, Z. S. Launer, and C. M. Patricola, 2008: Springtime intensification of the Great Plains low-level jet and Midwest precipitation in GCM simulations of the twenty-first century. *J. Climate*, **21**, 6321–6340, https://doi.org/10.1175/2008JCLI2355.1.

Dee, D., and Coauthors, 2011: The ERA-Interim reanalysis: Configuration and performance of the data assimilation system. *Quart. J. Roy. Meteor. Soc.*, **137**, 553–597, https://doi.org/10.1002/qj.828.

Demory, M.-E., P. L. Vidale, M. J. Roberts, P. Berrisford, J. Strachan, R. Schiemann, and M. S. Mizielinski, 2014: The role of horizontal resolution in simulating drivers of the global hydrological cycle. *Climate Dyn.*, **42**, 2201–2225, https://doi.org/10.1007/s00382-013-1924-4.

Dirmeyer, P. A., and K. L. Brubaker, 1999: Contrasting evaporative moisture sources during the drought of 1988 and the flood of 1993. *J. Geophys. Res.*, **104**, 19 383–19 397, https://doi.org/10.1029/1999JD900222.

——, and ——, 2007: Characterization of the global hydrologic cycle from a back-trajectory analysis of atmospheric water vapor. *J. Hydrometeor.*, **8**, 20–37, https://doi.org/10.1175/JHM557.1.

——, and J. L. Kinter III, 2010: Floods over the us midwest: A regional water cycle perspective. *J. Hydrometeor.*, **11**, 1172–1181, https://doi.org/10.1175/2010JHM1196.1.

——, K. L. Brubaker, and T. DelSole, 2009: Import and export of atmospheric water vapor between nations. *J. Hydrol.*, **365**, 11–22, https://doi.org/10.1016/j.jhydrol.2008.11.016.

Efron, B., and R. J. Tibshirani, 1994: *An Introduction to the Bootstrap*. CRC Press, 456 pp.

Ferguson, C., M. Pan, and T. Oki, 2018: The effect of global warming on future water availability: CMIP5 synthesis. *Water Resour. Res.*, **54**, 7791–7819, https://doi.org/10.1029/2018WR022792.

Findell, K. L., P. W. Keys, R. J. van der Ent, B. R. Lintner, A. Berg, and J. P. Krasting, 2019: Rising temperatures increase importance of oceanic evaporation as a source for continental

precipitation. *J. Climate*, **32**, 7713–7726, https://doi.org/10.1175/JCLI-D-19-0145.1.

Gimeno, L., and Coauthors, 2012: Oceanic and terrestrial sources of continental precipitation. *Rev. Geophys.*, **50**, RG4003, https://doi.org/10.1029/2012RG000389.

——, R. Nieto, A. Drumond, R. Castillo, and R. Trigo, 2013: Influence of the intensification of the major oceanic moisture sources on continental precipitation. *Geophys. Res. Lett.*, **40**, 1443–1450, https://doi.org/10.1002/grl.50338.

Guo, L., R. van der Ent, N. Klingaman, M. Demory, P. Vidale, A. Turner, C. Stephan, and A. Chevuturi, 2019: Moisture sources for East Asian precipitation: Mean seasonal cycle and interannual variability. *J. Hydrometeor.*, **20**, 657–672, https://doi.org/10.1175/JHM-D-18-0188.1.

Haarsma, R. J., and Coauthors, 2016: High resolution model intercomparison project (HighResMIP v1. 0) for CMIP6. *Geosci. Model Dev.*, **9**, 4185–4208, https://doi.org/10.5194/gmd-9-4185-2016.

——, W. Hazeleger, C. Severijns, H. de Vries, A. Sterl, R. Bintanja, G. J. van Oldenborgh, and H. W. van den Brink, 2013: More hurricanes to hit western Europe due to global warming. *Geophys. Res. Lett.*, **40**, 1783–1788, https://doi.org/10.1002/grl.50360.

Hazeleger, W., and Coauthors, 2010: EC-Earth: A seamless earth-system prediction approach in action. *Bull. Amer. Meteor. Soc.*, **91**, 1357–1363, https://doi.org/10.1175/2010BAMS2877.1.

——, and Coauthors, 2012: EC-Earth v2. 2: Description and validation of a new seamless earth system prediction model. *Climate Dyn.*, **39**, 2611–2629, https://doi.org/10.1007/s00382-011-1228-5.

Held, I. M., and B. J. Soden, 2006: Robust responses of the hydrological cycle to global warming. *J. Climate*, **19**, 5686–5699, https://doi.org/10.1175/JCLI3990.1.

Helfand, H. M., and S. D. Schubert, 1995: Climatology of the simulated great plains low-level jet and its contribution to the continental moisture budget of the United States. *J. Climate*, **8**, 784–806, https://doi.org/10.1175/1520-0442(1995)008<0784:COTSGP>2.0.CO;2.

Herrera-Estrada, J. E., J. A. Martinez, F. Dominguez, K. L. Findell, E. F. Wood, and J. Sheffield, 2019: Reduced moisture transport linked to drought propagation across north america. *Geophys. Res. Lett.*, **46**, 5243–5253, https://doi.org/10.1029/2019GL082475.

Higgins, R. W., Y. Yao, E. Yarosh, J. E. Janowiak, and K. Mo, 1997: Influence of the Great Plains low-level jet on summertime precipitation and moisture transport over the central United States. *J. Climate*, **10**, 481–507, https://doi.org/10.1175/1520-0442(1997)010<0481:IOTGPL>2.0.CO;2.

——, W. Shi, E. Yarosh, and R. Joyce, 2000: Improved United States precipitation quality control system and analysis. NCEP/Climate Prediction Center Atlas 7, NOAA, 40 pp., http://www.cpc.ncep.noaa.gov/research_papers/ncep_cpc_atlas/7/toc.html.

Hodges, K. I., R. W. Lee, and L. Bengtsson, 2011: A comparison of extratropical cyclones in recent reanalyses ERA-Interim, NASA MERRA, NCEP CFSR, and JRA-25. *J. Climate*, **24**, 4888–4906, https://doi.org/10.1175/2011JCLI4097.1.

Hoyos, I., F. Dominguez, J. Cañón-Barriga, J. Martínez, R. Nieto, L. Gimeno, and P. Dirmeyer, 2018: Moisture origin and transport processes in Colombia, northern South America. *Climate Dyn.*, **50**, 971–990, https://doi.org/10.1007/s00382-017-3653-6.

Knoche, H. R., and H. Kunstmann, 2013: Tracking atmospheric water pathways by direct evaporation tagging: A case study for West Africa. *J. Geophys. Res. Atmos.*, **118**, 12–345, https://doi.org/10.1002/2013JD019976.

Knutti, R., R. Furrer, C. Tebaldi, J. Cermak, and G. A. Meehl, 2010: Challenges in combining projections from multiple climate models. *J. Climate*, **23**, 2739–2758, https://doi.org/10.1175/2009JCLI3361.1.

Martens, B., and Coauthors, 2016: GLEAM v3: Satellite-based land evaporation and root-zone soil moisture. *Geosci. Model Dev.*, **10**, 1903–1925, https://doi.org/10.5194/gmd-10-1903-2017.

Murakami, H., and Coauthors, 2015: Simulation and prediction of category 4 and 5 hurricanes in the high-resolution GFDL HiFLOR coupled climate model. *J. Climate*, **28**, 9058–9079, https://doi.org/10.1175/JCLI-D-15-0216.1.

Nakićenović, N., and R. Swart, Eds., 2000: *Special Report on Emissions Scenarios*. Cambridge University Press, 570 pp.

Rogelj, J., M. Meinshausen, and R. Knutti, 2012: Global warming under old and new scenarios using IPCC climate sensitivity range estimates. *Nat. Climate Change*, **2**, 248–253, https://doi.org/10.1038/nclimate1385.

Seager, R., and N. Henderson, 2013: Diagnostic computation of moisture budgets in the ERA-Interim reanalysis with reference to analysis of CMIP-archived atmospheric model data. *J. Climate*, **26**, 7876–7901, https://doi.org/10.1175/JCLI-D-13-00018.1.

——, and Coauthors, 2007: Model projections of an imminent transition to a more arid climate in southwestern North America. *Science*, **316**, 1181–1184, https://doi.org/10.1126/science.1139601.

——, N. Naik, and G. A. Vecchi, 2010: Thermodynamic and dynamic mechanisms for large-scale changes in the hydrological cycle in response to global warming. *J. Climate*, **23**, 4651–4668, https://doi.org/10.1175/2010JCLI3655.1.

——, M. Ting, C. Li, N. Naik, B. Cook, J. Nakamura, and H. Liu, 2013: Projections of declining surface-water availability for the southwestern United States. *Nat. Climate Change*, **3**, 482–486, https://doi.org/10.1038/nclimate1787.

——, and Coauthors, 2014: Dynamical and thermodynamical causes of large-scale changes in the hydrological cycle over North America in response to global warming. *J. Climate*, **27**, 7921–7948, https://doi.org/10.1175/JCLI-D-14-00153.1.

Shaffrey, L. C., and Coauthors, 2009: U.K. HiGEM: The new U.K. high-resolution global environment model—Model description and basic evaluation. *J. Climate*, **22**, 1861–1896, https://doi.org/10.1175/2008JCLI2508.1.

Singh, H. K., C. M. Bitz, A. Donohoe, J. Nusbaumer, and D. C. Noone, 2016: A mathematical framework for analysis of water tracers. Part II: Understanding large-scale perturbations in the hydrological cycle due to CO_2 doubling. *J. Climate*, **29**, 6765–6782, https://doi.org/10.1175/JCLI-D-16-0293.1.

Sodemann, H., C. Schwierz, and H. Wernli, 2008: Interannual variability of Greenland winter precipitation sources: Lagrangian moisture diagnostic and North Atlantic Oscillation influence. *J. Geophys. Res.*, **113**, D03107, https://doi.org/10.1029/2007JD008503.

Sterl, A., and Coauthors, 2008: When can we expect extremely high surface temperatures? *Geophys. Res. Lett.*, **35**, L14703, https://doi.org/10.1029/2008GL034071.

Stohl, A., and P. James, 2005: A Lagrangian analysis of the atmospheric branch of the global water cycle. Part II: Moisture transports between Earth's ocean basins and river catchments. *J. Hydrometeor.*, **6**, 961–984, https://doi.org/10.1175/JHM470.1.

Strachan, J., P. L. Vidale, K. Hodges, M. Roberts, and M.-E. Demory, 2013: Investigating global tropical cyclone activity

with a hierarchy of AGCMs: The role of model resolution. *J. Climate*, **26**, 133–152, https://doi.org/10.1175/JCLI-D-12-00012.1.

Taylor, K. E., R. J. Stouffer, and G. A. Meehl, 2012: An overview of cmip5 and the experiment design. *Bull. Amer. Meteor. Soc.*, **93**, 485–498, https://doi.org/10.1175/BAMS-D-11-00094.1.

Trenberth, K. E., 1991: Climate diagnostics from global analyses: Conservation of mass in ecmwf analyses. *J. Climate*, **4**, 707–722, https://doi.org/10.1175/1520-0442(1991)004<0707:CDFGAC>2.0.CO;2.

——, 2011: Changes in precipitation with climate change. *Climate Res.*, **47**, 123–138, https://doi.org/10.3354/cr00953.

——, J. T. Fasullo, and J. Mackaro, 2011: Atmospheric moisture transports from ocean to land and global energy flows in reanalyses. *J. Climate*, **24**, 4907–4924, https://doi.org/10.1175/2011JCLI4171.1.

van den Hurk, B. J. J. M., P. Viterbo, and A. C. M. Beljaars, and A. K. Betts, 2000: Offline validation of the ERA40 surface scheme. ECMWF Tech Memo. 295, 42 pp., http://www.ecmwf.int/sites/default/files/elibrary/2000/12900-offline-validation-era40-surface-scheme.pdf.

van der Ent, R. J., 2014: A new view on the hydrological cycle over continents. Ph.D. thesis, Delft University of Technology, 106 pp., https://doi.org/10.4233/uuid:0ab824ee-6956-4cc3-b530-3245ab4f32be.

——, H. H. Savenije, B. Schaefli, and S. C. Steele-Dunne, 2010: Origin and fate of atmospheric moisture over continents. *Water Resour. Res.*, **46**, W09525, https://doi.org/10.1029/2010WR009127.

——, O. A. Tuinenburg, H.-R. Knoche, H. Kunstmann, and H. H. G. Savenije, 2013: Should we use a simple or complex model for moisture recycling and atmospheric moisture tracking? *Hydrol. Earth Syst. Sci.*, **17**, 4869–4884, https://doi.org/10.5194/hess-17-4869-2013.

——, L. Wang-Erlandsson, P. W. Keys, and H. Savenije, 2014: Contrasting roles of interception and transpiration in the hydrological cycle–Part 2: Moisture recycling. *Earth Syst. Dyn.*, **5**, 471–489, https://doi.org/10.5194/esd-5-471-2014.

van Heerwaarden, C. C., J. V.-G. de Arellano, and A. J. Teuling, 2010: Land-atmosphere coupling explains the link between pan evaporation and actual evapotranspiration trends in a changing climate. *Geophys. Res. Lett.*, **37**, L21401, https://doi.org/10.1029/2010GL045374.

Vannière, B., and Coauthors, 2019: Multi-model evaluation of the sensitivity of the global energy budget and hydrological cycle to resolution. *Climate Dyn.*, **52**, 6817–6846, https://doi.org/10.1007/s00382-018-4547-y.

van Vuuren, D. P., and Coauthors, 2011: The representative concentration pathways: An overview. *Climatic Change*, **109**, 5–31, https://doi.org/10.1007/s10584-011-0148-z.